J Electr Eng Technol.2015; 10(3): 1093-1101
http://dx.doi.org/10.5370/JEET.2015.10.3.1093

ISSN(Print) 1975-0102
ISSN(Online) 2093-7423

Partial Discharge Localization Based on Detailed Models of Transformer and Wavelet Transform Techniques

Seyed Mohammad Hassan Hosseini† and Peyman Rezaei Baravati*

Abstract – Partial Discharge (PD) is a physical phenomenon, which causes defects and damages to the insulation. This phenomenon is regarded as the most important source of fault and defect in power transformers. Therefore, methods of high speed and precision are considered of special importance for the maintenance of transformers in localization of the origin of partial discharge. In this paper, the transformer winding is first modeled in a transient state by using RLC ladder network and multi-conductor transmission line (MTL) models. The parameters of the two models were calculated by Ansoft Maxwell software, and the simulations were performed by Matlab software. Then, the PD pulses were applied to the models with different widths of pulses. With regard to the fact that the signals received after the application of PD had a variable frequency nature over time, and based on the wavelet transform and signal energy, a new method was presented for the localization of PD. Ultimately; the mentioned method was implemented on a 20 kV winding distribution transformer. Then, the performances of the models used in this paper, including RLC and MTL models, were compared in different frequency bands for the correct distinction of partial discharge location.

Keywords: Wavelet transform, Power transformer, RLC model, Multi-conductor transmission line (MTL), Partial discharge, PD localization.

1. Introduction

Power transformer is the most important unit in the power system both economically and functionally. Therefore it is highly necessary to know the real conditions of transformer insulation to increase the reliability. On the other hand, the function and life span of transformer insulation is highly affected by partial discharge. Proper recognition and also PD localization help us to prevent terrible incidents in power system. Methods of PD localization and calculating can be classified in to two groups of electrical and non-electrical methods based on the effects that PD can cause in an insulator. [1]. Non-electrical methods are also categorized into three methods: Audio, chemical and optical by which the presence or absence of partial discharge in the insulator can only be realized. Electrical methods are the most successful and practical methods in localization and calculation of PD. Among electrical methods, methods which are based on transformer modeling are used for PD localization in transformers. In these methods, transformer winding is modeled in high frequencies based on the available information from designing of transformer [2].

According to the studies done in this respect, we can mention three models: the traveling wave model [3] multi-conductor transmission line model (MTL) [4] and RLC ladder network [5].

After winding modeling, electrical PD pulses are injected in different parts of the winding and the created signals are recorded in terminals. Localization is then done after analyzing the recorded signals. PD localization is done in different ways such as: Transfer Function based on partial discharge localization [6], PD localization based on zeros and poles of frequency spectrum [7] and PD localization based on pattern recognition [8]. In most of the presented methods, PD localization is full of errors due to the weakness in precise winding modeling and invalid processing algorithm in high frequencies. Hence, in this paper, a valid algorithm is presented using the wavelet transform (WT) in order to find a suitable location for PD in the transformer winding in offline state by precise modeling of transformer winding and calculation of parameters with high accuracy using finite elements method (FEM) in Ansoft Maxwell software.

This paper consists of six parts. In the second part, precisely introduce the RLC and multi-conductor transmission line models, and in the third part, wavelet transforms and Parseval's theorem are described. Modeling methods and suggested algorithm simulation on 20 kV winding are also illustrated in the fourth part. In the fifth section, the laboratory results of the above method are implemented on the practical model and a comparison is made between the results of localization obtained from the RLC model and those of multi-conductor transmission line model, and the conclusion is presented in section six.

† Corresponding Author: Dept. of Electrical Engineering, South Tehran Branch, Islamic Azad University, Tehran, Iran. (Smhh110@azad.ac.ir)
* Dept. of Electrical Engineering, South Tehran Branch, Islamic Azad University, Tehran, Iran. (Peyman.rezaei@gmail.com)
Received: April 21, 2014; Accepted: November 25, 2014

2. High-frequency Models of Transformer Winding

To study the manner of partial discharge behavior in the transformer winding, there is a need for an accurate modeling of the transformer winding. There are different methods to model the transformer winding. So far, the RLC models and multi-conductor transmission lines (MTL) by which the set of transformer windings can be physically studied and evaluated have been introduced. The RLC model is a circuit with integrated elements and a limited number of nodes. As a result, the frequency validity limit is limited up to about one MHz. Precision in calculating the numeric value of the parameters of the model that is self and mutual inductance and capacitance has a great effect in reducing the errors of simulation and PD localization. In this model each unit of transformer is modeled with an R, L, and C network. Fig. 1 shows the transformer winding RLC model.

In Fig. 1, L_i is self-inductance of i unit, M_{ij} is mutual inductance of i and j units. K_i is capacitance for i unit, C_i is the capacitance between i unit and earth potential (core or tank), G_s is conductance which is representing the dielectric loss of the i unit, G_g is conductance which is representing the dielectric loss of the i unit and earth and r is the ohmic resistance indicating ohmic losses of the i unit.

The multi-conductor transmission line model enjoys higher frequency validity limit contrary to the RLC and can predict the wavy behavior of high-frequency effects. In this model, the winding parameters are considered extensively and the winding behavior is described by transmission line equations; also, each turn of the transformer winding is modeled as one single-conductor transmission line with an equivalent circuit similar to Fig. 2. The equations of transmission lines in time domain can be written as follows:

$$\frac{\partial\left[U(x,t)\right]}{\partial x}=-\left([R]\left[I(x,t)\right]+[L]\frac{\partial\left[I(x,t)\right]}{\partial t}\right) \quad (1)$$

$$\frac{\partial\left[I(x,t)\right]}{\partial x}=-\left([G]\left[U(x,t)\right]+[C]\frac{\partial\left[U(x,t)\right]}{\partial t}\right) \quad (2)$$

Where in Eqs. (1) and (2), L is the inductance, R is the resistance, C is the capacitor capacitance, and G is the parallel resistance of a small part of the transmission line [9]. Also in Fig. 2, U_S and I_S are the voltage vectors and the current transmitted from the beginning of the transmission line, respectively. U_R and I_R are the voltage and current vectors, respectively received at the end of the transmission line.

Applying analytical formula to calculate these parameters especially self and mutual inductance is a complex and time-consuming process. Therefore in most of the studies done so far the modeling for each unit of winding, R, L, C values are calculated; these values are then considered for other units. Mutual inductances that exist between different turns of each winding are also ignored which cause errors in modeling and PD localization. One of the best methods to calculate the parameters of detailed models is applying the finite element method (FEM) by Ansoft Maxwell software [10, 11]. This paper has made use of this method to calculate the exact amount of parameters such as mutual inductances.

Modeling of winding, precision of the parameters obtained, and the manner of the propagation of partial discharge signal by using RLC and MTL models are fully presented in references [10, 11]. In reference [2], a comparison is made among the detailed models of the transformer for the purpose of studying the transient state, and it has been shown that the frequency credit range of RLC model, 10kHz < f < 1MHz and the multi-conductor transmission line model is 1MHz ≤ f ≤ 5 MHz. To localize the partial discharge in the transformer winding, the detailed models are employed in this paper, and by using wavelet transform techniques, the location of PD is estimated in two models. Ultimately, the frequency validity limit of the transformer detailed models has been studied by using the proposed algorithm in localizing PD.

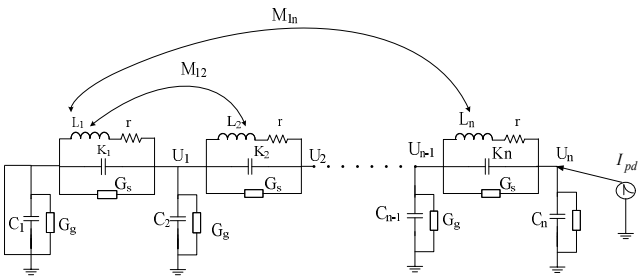

Fig. 1. Winding equivalent circuit inform R, L, C Ladder network.

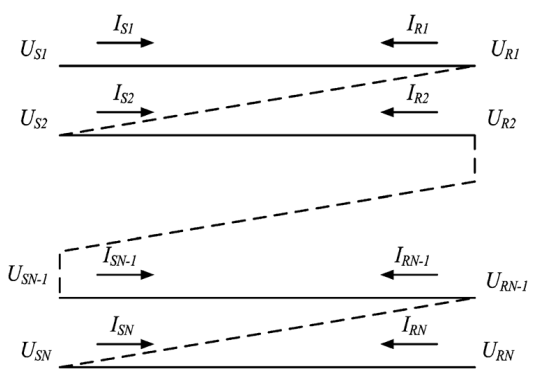

Fig. 2. Multi-conductor transmission line model

3. Wavelet Transform

Wavelet transform is a scale-time transform saving the data of the two domains of time and frequency. The

transform of wavelet is of two types of continuous (CWT) and discrete (DWT). Here also due to the time-consuming calculation of CWT coefficients in computer applications, the DWT is used. Therefore, the discrete wavelet transform for X(t) signal is defined as follows:

$$DWT(j,k)=\frac{1}{\sqrt{s}}\int_{-\infty}^{+\infty} x(t)\,\Psi^{*}\left(\frac{t-k\tau_0 s^{j}{}_0}{s^{j}{}_0}\right) \tag{3}$$

In equation (3), x(t) and Ψ are the initial signal and wavelet function, respectively. Also, $k\tau_0\ s^{j}{}_0$ is the transform parameter, $s^{j}{}_0$ is the scale parameter and j shows level of wavelet transform. Among various types of wavelet discretization, binary discretization with S_0=2 and τ_0=1 is widely used. Discrete wavelet transform can be achieved well with a pair of low- pass and high-pass filter which is shown as L(K) and H(K) respectively. By using these filters, x(n) discrete signal decomposes in to high frequency and low frequency. When the components of high and low frequency are decomposed, the low frequency wavelet is only used in the next step. CA_1 and CD_1 are approximation coefficient and detail coefficient of x(n) signal in first level respectively and are calculated based on (4) and (5):

$$CA_1=\sum_{k}^{n} L(k-2n)\,x(k) \tag{4}$$

$$CD_1=\sum_{k}^{n} H(k-2n)\,x(k) \tag{5}$$

It is worth noting that the number of needed levels for discrete wavelet transform depends on the frequency characteristics of the signals under analysis. Finally discrete wavelet transform of the signal is calculated by gathering the output filters. Fig. 3, shows how to calculate the 3 level discrete wavelet transform by using the idea of filter bank for a x(n) desired signal.

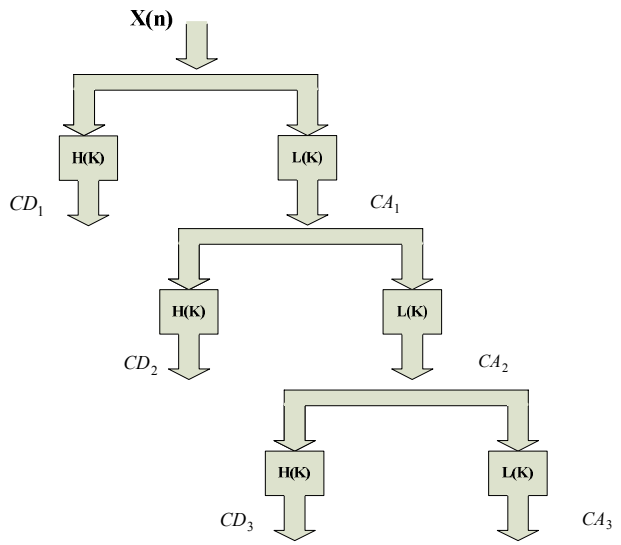

Fig. 3. Decomposition of the signal in DWT

3.1 Parseval's Theorem

In order to make the energy vectors small, energy of various levels of wavelet transform is used instead of wavelet transform coefficients. For this reason, we've made use of Parseval's theorem. Parseval's relation is:

$$\frac{1}{N}\sum_{n=<N>}\left|x[n]\right|^2=\sum_{k=<n>}\left|a_k\right|^2 \tag{6}$$

Where N is the sampling period, and a_k is the spectrum coefficients of the Fourier transform.

The signal energy can be obtained from relation (7):

$$\frac{1}{N}\sum_{t}\left|x[t]\right|^2=\frac{1}{N_J}\sum_{k}\left|cA_{j,k}\right|^2+\sum_{j=1}^{J}\left(\frac{1}{N_j}\sum_{k}\left|cD_{j,k}\right|^2\right) \tag{7}$$

In this relation, $CA_{j,k}$ equals approximation coefficients, $CD_{j,k}$ equals detail coefficients in j scale, N is the number of samples in the input signal, N_j is the number of samples at any analysis level and J is the number of analysis levels. In the right hand side of this relation, the energy is related to the high frequency and low frequency elements. Also, the left side of this relation indicates the whole signal energy.

With regard to the application of Parseval's theorem in the analysis of discrete wavelet, the signals can be classified with regard to how energy is distributed in the high frequency and low frequency elements. P_a the energy distribution in low frequency elements and P_d the distribution of energy in high frequency elements are calculated from relations (8) and (9):

$$P_a=\frac{1}{N_j}\sum_{k}\left|cA\right|^2=\frac{\left\|cA\right\|^2}{N_j} \tag{8}$$

$$P_d=\frac{1}{N_j}\sum_{k}\left|cD_{j,k}\right|^2=\frac{\left\|cD_j\right\|^2}{N_j} \tag{9}$$

4. PD Localization Algorithm

The winding under study in this paper is related to the 20 kV transformers the details of whose dimensions have been mentioned in Table 1. The winding experimented in this paper was modeled and simulated by using RLC ladder network and MTL model along with the parameters obtained from FEM with the help of Matlab software. After modeling the transformer winding, it is necessary to enforce the partial discharge pulse to the winding. Hence, it is necessary to obtain the mathematical model of partial discharge pulse. Real PD pulses can be illustrated by

Table 1. The basic characteristics of the 20 kV transformer winding

Transformer 20kV-winding parameters	
Type of winding	Layer
Number of winding turns	38 turns
Diameter of winding	260 mm
Height of winding	160 mm
Width of conductor	8 mm
Height of conductor	2 mm

combining two exponential functions as follows:

$$pd(t) = \exp\left(-\frac{t}{p}\right) - \exp\left(-\frac{2t}{q}\right) \quad (10)$$

Where, p and q are first and second time constants, respectively, so that p≥q. By changing the p and q quantities, the rise time and pulse width can be changed.

Based on this, with the help of Matlab software, signals with varied ranges were produced and enforced in various points of the winding in two models. Having the quantities of transfer functions and impulse supposition for the partial discharge current using relations (11) and (12), we can obtain the voltage amounts in the beginning and in the end of the winding for various quantities of injection locations of partial discharge pulse in the two models of RLC and MTL [5,11].

$$TF_L = \frac{V}{I_{PD}} \quad (11)$$

$$TF_N = \frac{V'}{I_{PD}} \quad (12)$$

Where, The transfer function from PD source to the line-end (TF_L), the transfer function from PD source to the neutral-end (TF_N). V and V' are beginning and end of winding voltages, respectively and I_{PD} is the PD pulse current.

Then, for PD localization based on the proposed algorithm, the first step is the application of PD pulse on each round of the windings. Fig. 4 shows the manner of the application of the PD pulse and storage of the voltage signal.

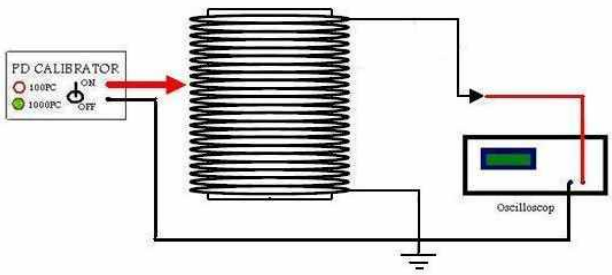

Fig. 4. The circuit of the application of a partial discharge signal on the sample winding.

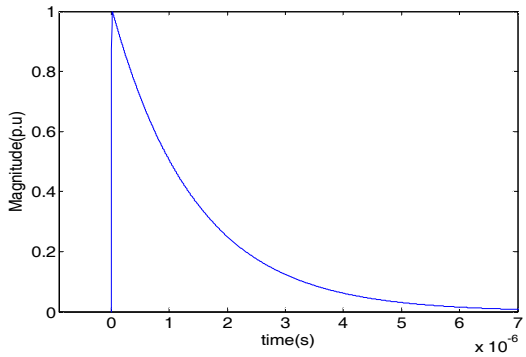

Fig. 5. PD pulse with 20ns rise time and 1μs width.

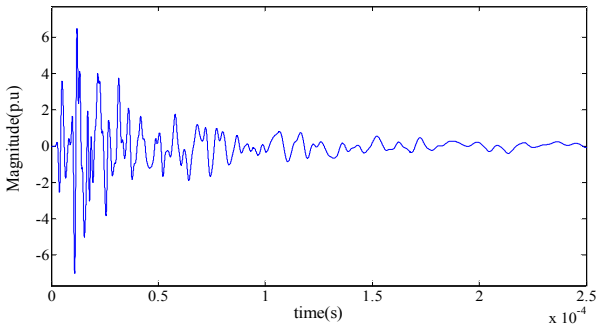

Fig. 6. Representation of V_{10}(t) signal in RLC model.

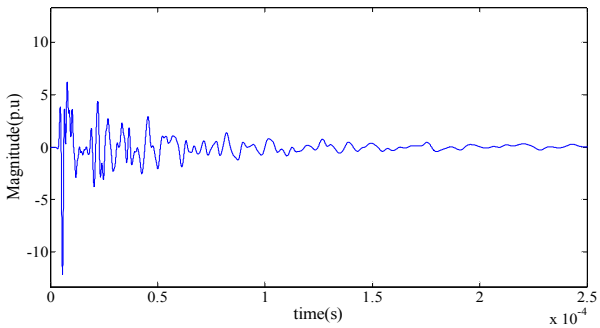

Fig. 7. Representation of V_{10}(t) signal in MTL model.

Consider a reference PD pulse with 20ns rise time and 1μs width like Fig. 5. This pulse is similar to the specifications and results obtained from laboratory tests.

This pulse is injected to the first turn of winding and its corresponding response i.e. V_1 (t) is measured. In this way, this is repeated for all the 38 turn of winding and their corresponding voltages V_2 (t) to V_{38} (t) are recorded.

By doing this, a database of the winding response to the injection of the PD pulse in different locations and in two models of RLC and multi-conductor transmission line is obtained. For example, Figs. 6 to 9 show the V_{10}(t) and V_{14} (t) signals for two models of RLC and multi-conductor transmission line, respectively.

In the third step, it is assumed that PD is occurred in an unknown location of the winding, for this purpose, another PD pulse with different specification like 0.35μs rise time and 1.15μs width is injected to one of the winding turn just like the turn number m^{th} and U_m (t) is recorded.

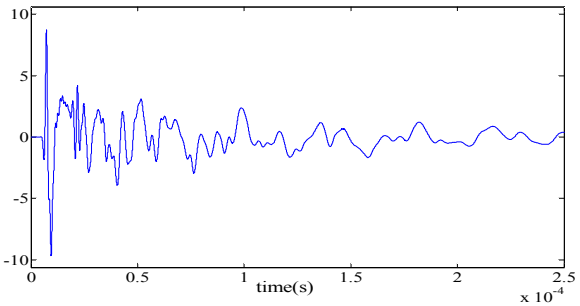

Fig. 8. Representation of $V_{14}(t)$ signal in RLC model.

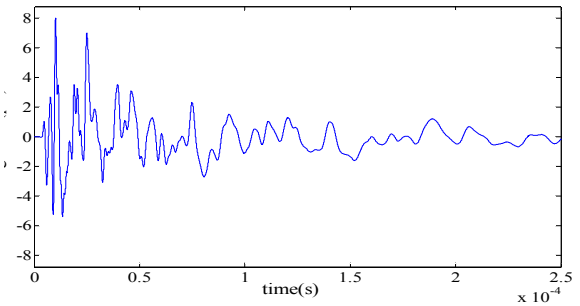

Fig. 9. Representation of $V_{14}(t)$ signal in MTL model.

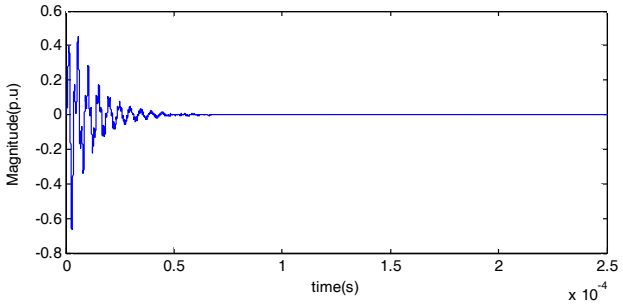

Fig. 10. Representation of $U_{14}(t)$ signal in RLC model.

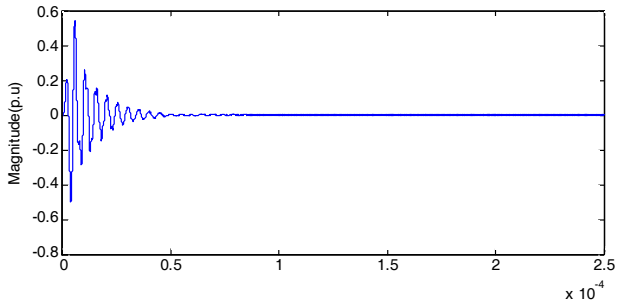

Fig. 11. Representation of $U_{14}(t)$ signal in MTL model.

For example, Figs. 10 and 11 show the $U_{14}(t)$ voltage, which is the response of the winding after the application of the above PD pulse to the 14th turn in two models.

Comparing $U_m(t)$ and database in the suggested method, we are looking for a way to determine in which turns PD occurs.

Since the frequency content of the recorded voltages varies with time, in the fourth step of $V_1(t)$ to $V_{38}(t)$ signals and also $U_m(t)$ signal, the discrete wavelet transform is

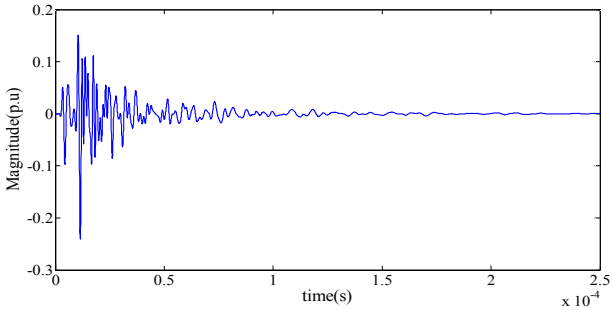

Fig. 12. Representation of Detail coefficients of first level for $V_{10}(t)$ signal in RLC model.

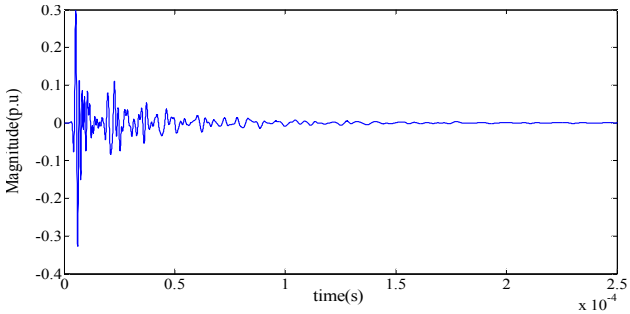

Fig. 13. Representation of Detail coefficients of first level for $V_{10}(t)$ signal in MTL model.

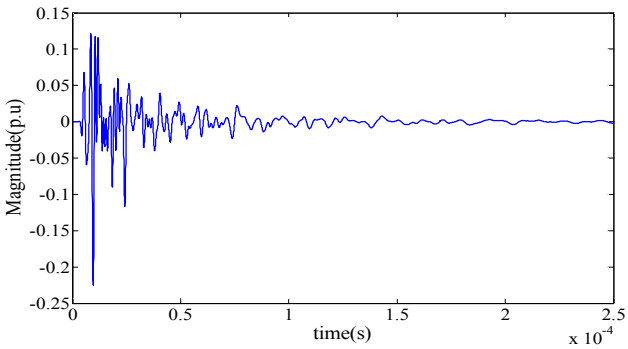

Fig. 14. Representation of Detail coefficients of first level for $V_{14}(t)$ signal in RLC model.

considered separately and at the first level.

Mother wavelet function which is used in this step is (Daubechies 1) db1. This is for similarity of recorded signals by db1 mother wavelet function. Getting a wavelet transform, each signal is divided in to two components. One of them is detailed component which includes high frequency; the other one is approximate component which includes low frequency. So, for PD identification, detailed component which includes high frequencies must be analyzed. For example Figs. 12 to 15, show the Detail coefficient of first level for V_{10} (t) and V_{14} (t) signals. Also Figs. 16 and 17, display the Detail coefficient of first level for U_{14} (t) signal.

In the fifth step, the correlation between detail Coefficient vector of U_m (t) signal and detail Coefficient vector of V_1 (t) signal is calculated. The energy of the

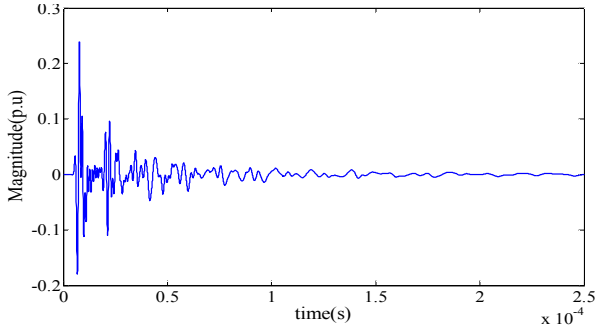

Fig. 15. Representation of Detail coefficients of first level for $V_{14}(t)$ signal in MTL model.

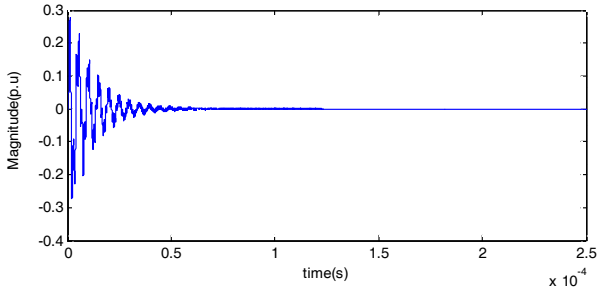

Fig. 16. Representation of Detail coefficients of first level for $U_{14}(t)$ signal in RLC model.

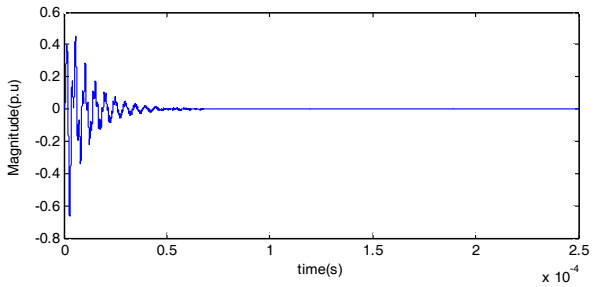

Fig. 17. Representation of Detail coefficients of first level for $U_{14}(t)$ signal in MTL model.

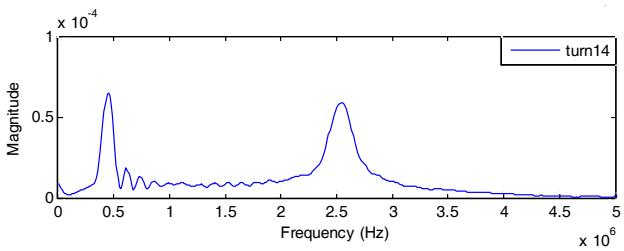

Fig. 18. Frequency spectrum of $V_{14}(t)$ signal.

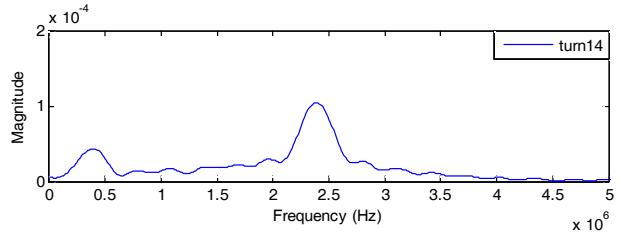

Fig. 19. Frequency spectrum of $U_{14}(t)$ signal.

vector resulting from this correlation is then calculated by the use of Parseval's theorem. This process has also been repeated for wavelet transform output of V_2 (t) to V_{38} (t). For PD localization, we are looking for a $V_n(t)$ which

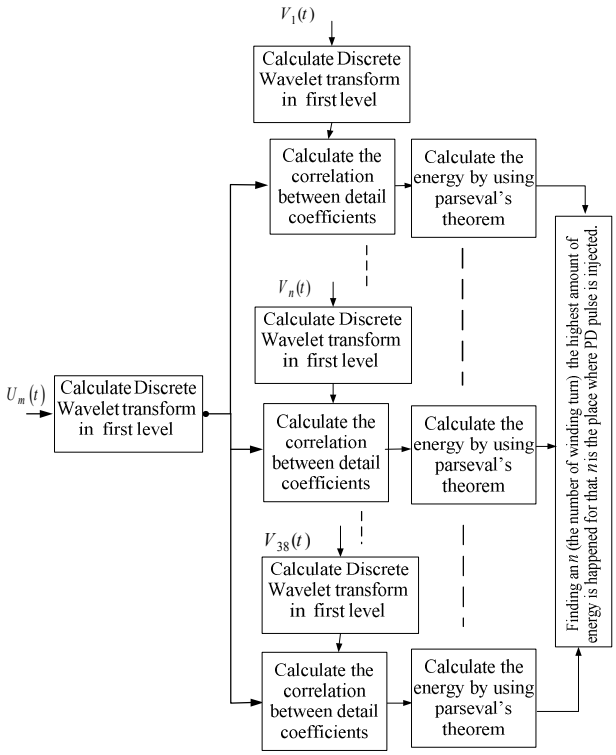

Fig. 20. Different steps of proposed algorithm for localization of PD.

Table 2. Result of calculation of energy obtaining from correlation of detail coefficients between DWT ($U_{14}(t)$), and DWT ($V_1(t)$) to DWT ($V_{38}(t)$) signals in RLC model. These results are also repeated for $U_{20}(t)$ signals. (Numbers are based on Micro Joule)

	V_1	V_2	V_3	V_4	V_5	V_6
U_{14}	0.0373	0.0394	0.1042	0.0796	0.0445	0.0608
U_{20}	0.033	0.034	0.045	0.074	0.037	0.035
	V_7	V_8	V_9	V_{10}	V_{11}	V_{12}
U_{14}	0.1622	0.1614	0.1630	0.3671	0.6761	0.5346
U_{20}	0.167	0.163	0.06	0.415	0.789	0.436
	V_{13}	V_{14}	V_{15}	V_{16}	V_{17}	V_{18}
U_{14}	0.2689	**0.7353**	0.6045	0.4639	0.3042	0.3686
U_{20}	0.161	0.576	0.661	0.415	0.438	0.703
	V_{19}	V_{20}	V_{21}	V_{22}	V_{23}	V_{24}
U_{14}	0.2830	0.2446	0.2407	0.2499	0.0869	0.0856
U_{20}	0.818	**1.128**	0.561	0.688	0.198	0.305
	V_{25}	V_{26}	V_{27}	V_{28}	V_{29}	V_{30}
U_{14}	0.0618	0.0492	0.0516	0.0501	0.0581	0.0489
U_{20}	0.14	0.278	0.127	0.17	0.176	0.123
	V_{31}	V_{32}	V_{33}	V_{34}	V_{35}	V_{36}
U_{14}	0.0296	0.0272	0.0408	0.0133	0.0243	0.0885
U_{20}	0.075	0.086	0.069	0.042	0.05	0.148
	V_{37}	V_{38}				
U_{14}	0.0101	0.0822				
U_{20}	0.028	0.142				

Table 3. Result of calculation of energy obtaining from correlation of detail coefficients between DWT ($U_{14}(t)$), and DWT ($V_1(t)$) to DWT ($V_{38}(t)$) signals in MTL model. These results are also repeated for U_{20} (t) signals. (Numbers are based on Micro Joule)

	V_1	V_2	V_3	V_4	V_5	V_6
U_{14}	0.0596	0.0942	0.1321	0.0688	0.0542	0.0636
U_{20}	0.0294	0.0289	0.0304	0.0492	0.0522	0.0326
	V_7	V_8	V_9	V_{10}	V_{11}	V_{12}
U_{14}	0.1456	0.1571	0.1771	0.4321	0.5383	0.5219
U_{20}	0.0690	0.1008	0.1335	0.2299	0.5005	0.4038
	V_{13}	V_{14}	V_{15}	V_{16}	V_{17}	V_{18}
U_{14}	0.7386	**0.8147**	0.6279	0.5219	0.3318	0.3360
U_{20}	0.3209	0.5527	0.5761	0.5486	0.4996	0.7517
	V_{19}	V_{20}	V_{21}	V_{22}	V_{23}	V_{24}
U_{14}	0.3339	0.2665	0.2374	0.2094	0.1981	0.0760
U_{20}	0.8337	**0.8699**	0.6240	0.6153	0.4514	0.2461
	V_{25}	V_{26}	V_{27}	V_{28}	V_{29}	V_{30}
U_{14}	0.0715	0.0464	0.0445	0.0669	0.0620	0.0358
U_{20}	0.2606	0.2144	0.2083	0.1629	0.1692	0.0986
	V_{31}	V_{32}	V_{33}	V_{34}	V_{35}	V_{36}
U_{14}	0.0377	0.0326	0.0515	0.0287	0.0179	0.0138
U_{20}	0.0936	0.0921	0.0844	0.1417	0.0420	0.0667
	V_{37}	V_{38}				
U_{14}	0.0149	0.0741				
U_{20}	0.0155	0.0811				

maximum energy has happened for that. In this way, n is the turn in which PD is occurred and by doing this, PD is localized. The proposed algorithm is shown briefly in the Fig. 20. Tables 2 and 3 represents the results of simulation for $U_{14}(t)$ signal in two models of RLC and MTL. The numbers shown in Tables 2 and 3 express the value of energy. As it is specified in the tables, the maximum amount of energy has occurred for $V_{14}(t)$ Therefore, PD occurs in the 14th turn of winding.

All the mentioned steps are also repeated for 20th turn, and the results in Tables 2 and 3 indicate the success of the proposed algorithm in the two models. Also, in Figs. 18 and 19, frequency spectrum of $V_{14}(t)$ and $U_{14}(t)$ signals has been shown.

5. Laboratory Results

The proposed algorithm was implemented on the practical sample in laboratory environment. Fig. 21 shows 20 kV winding which is under examination.

Since the above winding has 38 turns, the partial discharge pulse was injected into different points of the winding by PD Calibrator. The partial discharge signals were measured and the frequency range, discharge time duration as well as the amplitude value of this signal was recorded. These signals were injected into the winding under experimentation within the frequency range of kHz to MHz. First, we injected a PD pulse with specifications in Fig. 5 into the first to thirty-eighth turns, and the

Fig. 21. The tested distribution 20 kV transformer winding

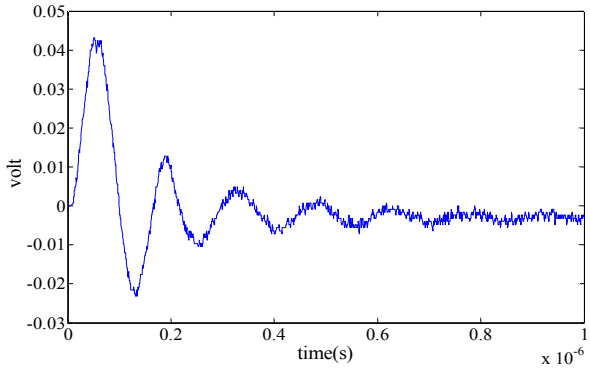

Fig. 22. Representation of V_1 (t) signal relevant to the practical example recorded in lab setting.

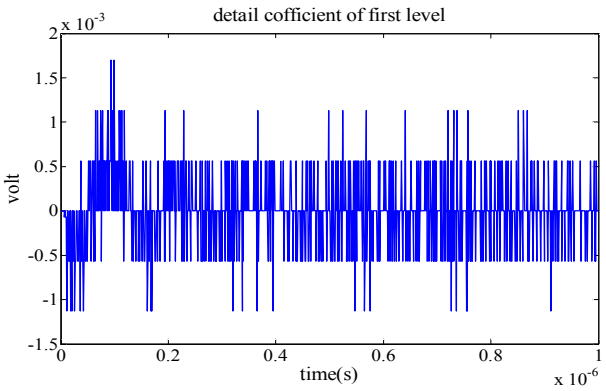

Fig. 23. Representation of Detail coefficients of first level for $V_1(t)$ signal relevant to the practical example recorded in lab setting.

response signals of $V_1(t)$ to $V_{38}(t)$ were measured and stored by an oscilloscope. For example, Fig. 22 shows the voltage signal $V_1(t)$ resulting from the application of PD pulse to the first turn, and Fig. 23 shows the detail coefficients of wavelet transform of this signal in the first level.

In the next section, another PD signal with different amplitude was injected into one of the winding turns e.g. the 11th turn and the response signal was stored again. The results of PD localization by using the proposed algorithm on the 20 kV winding are presented in Table 4. Localization based on RLC model and the injected PD frequency components are within the range of kHz.

Table 4. Result of the calculation of the energy obtaining from the correlation of detail coefficients between DWT (U_{11} (t)), and DWT (V_1 (t)) to DWT (V_{38}(t)) signals in RLC model within the frequency range of 100 kHz < f < 1MHz. (Numbers are based on Micro Joule)

	V_1	V_2	V_3	V_4	V_5	V_6
U_{11}	0.0319	0.0363	0.0105	0.0892	0.0869	0.0584
	V_7	V_8	V_9	V_{10}	V_{11}	V_{12}
U_{11}	0.1907	0.2177	0.3552	0.5008	**0.6386**	0.5111
	V_{13}	V_{14}	V_{15}	V_{16}	V_{17}	V_{18}
U_{11}	0.3335	0.5235	0.5584	0.4123	0.4010	0.4063
	V_{19}	V_{20}	V_{21}	V_{22}	V_{23}	V_{24}
U_{11}	0.3367	0.3449	0.3196	0.2320	0.0990	0.0972
	V_{25}	V_{26}	V_{27}	V_{28}	V_{29}	V_{30}
U_{11}	0.0584	0.0629	0.0347	0.0422	0.0374	0.0345
	V_{31}	V_{32}	V_{33}	V_{34}	V_{35}	V_{36}
U_{11}	0.0291	0.0285	0.0189	0.0112	0.0267	0.0149
	V_{37}	V_{38}				
U_{11}	0.0087	0.0180				

Table 5. Result of the calculation of the energy obtaining from the correlation of detail coefficients between DWT (U_{11} (t)), and DWT (V_1 (t)) to DWT (V_{38}(t)) signals in RLC model within the frequency range of f ≤ 5MHz. (Numbers are based on Micro Joule)

	V_1	V_2	V_3	V_4	V_5	V_6
U_{11}	0.0403	0.0873	0.1175	0.2596	0.4245	0.6018
	V_7	V_8	V_9	V_{10}	V_{11}	V_{12}
U_{11}	0.6771	0.7320	0.7336	**0.7405**	0.7277	0.6848
	V_{13}	V_{14}	V_{15}	V_{16}	V_{17}	V_{18}
U_{11}	0.5471	0.6062	0.5957	0.4925	0.4340	0.3241
	V_{19}	V_{20}	V_{21}	V_{22}	V_{23}	V_{24}
U_{11}	0.1873	0.1851	0.2180	0.2307	0.0731	0.1069
	V_{25}	V_{26}	V_{27}	V_{28}	V_{29}	V_{30}
U_{11}	0.0437	0.0488	0.0312	0.0532	0.0492	0.0408
	V_{31}	V_{32}	V_{33}	V_{34}	V_{35}	V_{36}
U_{11}	0.0334	0.0362	0.0488	0.0149	0.0198	0.0712
	V_{37}	V_{38}				
U_{11}	0.0755	0.0144				

As it is observed in Table 4, the maximum value is devoted to V_{11}(t). As a result, PD has occurred in the 11th turn and the PD location has been correctly estimated.

Next, the algorithm was also repeated for the injected PD frequency components within the Megahertz limit and the localization results were presented in Tables 5 and 6. As observed in Table 5, localization has estimated the location of PD with a minor error by using RLC model, which is due to the limitation of frequency range of RLC model in the range of megahertz. In order to solve this problem, and to obtain more precise results, localization has been studied based on multi-conductor transmission line (MTL). The results are presented in Table 6. As it is observed, since the maximum value is devoted to V_{11}(t), PD is estimated in the 11th turn. The evaluation of the results obtained from

Table 6. Result of the calculation of the energy obtaining from the correlation of detail coefficients between DWT (U_{11} (t)), and DWT (V_1 (t)) to DWT (V_{38}(t)) signals in MTL model within the frequency range of f ≤ 5MHz. (Numbers are based on Micro Joule)

	V_1	V_2	V_3	V_4	V_5	V_6
U_{11}	0.0376	0.0369	0.0931	0.0775	0.0581	0.0536
	V_7	V_8	V_9	V_{10}	V_{11}	V_{12}
U_{11}	0.2883	0.1789	0.1741	0.3791	**0.4014**	0.3440
	V_{13}	V_{14}	V_{15}	V_{16}	V_{17}	V_{18}
U_{11}	0.3242	0.3287	0.3340	0.264	0.3145	0.3012
	V_{19}	V_{20}	V_{21}	V_{22}	V_{23}	V_{24}
U_{11}	0.235	0.3192	0.3043	0.1517	0.0923	0.0932
	V_{25}	V_{26}	V_{27}	V_{28}	V_{29}	V_{30}
U_{11}	0.1566	0.0542	0.0525	0.1558	0.0683	0.0356
	V_{31}	V_{32}	V_{33}	V_{34}	V_{35}	V_{36}
U_{11}	0.0183	0.0309	0.0373	0.0117	0.0368	0.0741
	V_{37}	V_{38}				
U_{11}	0.0062	0.0641				

the Tables shows that the PD localization by using the proposed algorithm determines the real location of PD along the length of the winding through appropriate estimation. Comparison of the results in Tables 4 to 6 showed better functioning of RLC model within the frequency range of kilohertz, and the MTL model within the frequency range of megahertz by using the proposed algorithm.

As it was observed, partial discharge is the most important source of error in transformer insulation. Therefore, the study of this phenomenon is very important. But, with regard to the frequency ranges of the partial discharge phenomenon, it should be said that the base of the correct and acceptable localization of partial discharge pulses in transformers is modeling the winding at high frequencies. It has also been shown in this paper that if the model employed within the frequency interval of the bandwidth of the PD measuring system is valid, good results will be obtained for PD localization.

6. Conclusion

With regard to the importance of localization of the partial discharge in transformers due to economic issues, and its greater longevity, proposing a fast, suitable, and secure method for the recognition of the PD location in the transformer winding seems necessary. Almost in all previous papers the both two terminal currents of the transformer winding are analyzed. For example in [7] the signals of both ends of the winding are registered and then using them, the two transfer functions between the PD location and the both terminals of the winding are obtained. It is shown that the zeros of these transfer functions differ when the location of the PD varies. But the proposed method in this paper is really simple and is also easily

applicable because the wavelet packets toolbox is accessible in Matlab software and it has been shown that by taking voltage samples from the beginning of the winding and studying and analyzing the detail component obtained from the wavelet transform of these samples which include the partial discharge pulses, the location of PD is identified.

Therefore, in this paper, the 20 kV winding of the distribution transformer was first simulated and modeled with Matlab software by using RLC and the multi-conductor transmission line models; and then, a new method for the localization of PD in the transformer winding was presented by using discrete wavelet transmission. It was also shown that if an unidentified PD signal were measured in the outlet ends of the winding, we could specify the location for the PD pulse injection by using wavelet transform and the energy resulting from the correlation of wavelet coefficients. This method was implemented for PD pulses with different widths to include the random nature of the PD. Hence, this method is considered a suitable and offline one in order to determine the location for the partial discharge in the power transformer. The proposed algorithm was studied through both simulation and experiment on a real 20 kV winding. The results showed the proposed method success and better functioning of the RLC model in frequency ranges under 1 MHz ($f < 1MHz$) and the MTL model in frequency range of MHz ($f \leq 5MHz$) by using the proposed algorithm.

References

[1] Junfeng Gui, Wensheng Gao, Kexiong Tan and Shengyou Gao "Locating Partial Discharge in Power Transformer by Electrical Method," Proc. Int. Conf. on Properties and Applications of Dielectric Materials, Vol. 1, pp. 459-462, 2003.

[2] S.M.H. Hosseini, M. Vakilian and G.B. Gharepetian, "Comparision of Transformer Detailed models for fast and veryfast transient Studies" IEEE Trans. on Power Delivery, Vol. 23, No. 2, pp. 733-741, 2008.

[3] Z.D. Wang, P.A.Crossley, K.J. Cornik, and D.H. Zho, "An Algorithm for Partial Discharge Location in Distribution Power Transformer", IEEE Power Engineering Society Winter Meeting, Vol. 3, pp. 2217-2222, 2000.

[4] M. Jafari and A. Akbari, "Partial discharge localization in transformer windings using multiconductor transmission line model," Elsevier Elecr. Power Syst. Res., Vol. 78, No. 6, pp. 1028-1037, 2008.

[5] A. M. Jafari, A. Akbari and M. Kharezi, "Partial Discharge Localization in Transformers Using Detailed Modeling of Winding and Calibration Pulses" Proc. Int. Conf. on Solid Dielectrics, pp. 536-539, 2007.

[6] Akbari, P. Werle, H. Borsi and E. Gockenbach, "Transfer Function-Based Partial Discharge Localization in Power Transformers A Feasibility Study", IEEE Electrical Insulation Magazine, Vol. 18, No. 5, pp. 22-33.2002.

[7] S. N. Hettiwatte, Z. D. Wang and P. A. Crossley, "Investigation of propagation of partial discharges in power transformers and techniques for locating the discharge", IEE Proc. Sci., Meas. Techn., Vol. 152, pp. 25-30, 2005.

[8] M. Homaei, A. M. Jafari and A. Akbari "Investigating Suitable Features for Partial Discharge Localization in Power Transformer" Proc. Int. Conf. on Condition Monitoring and Diagnosis, pp. 923-926, 2008.

[9] M. Popov, L. van der Sluis, R.P.P. Smeets, J.L. Roldan, "Analysis of Very Fast Transients in Layer-Type Transformer Windings" IEEE Trans.on Power Delivery, Vol.22, pp. 238-247, 2007.

[10] S. M. H. Hosseini, M. vakilian, "Using finite element method in calculation of parameters of transformer winding detailed model for partial discharge research" Turkish Journal of Electrical Engineering & Computer Sciences .2013.

[11] S. M. H. Hosseini, Peyman Rezaei Baravati, "Transformer Winding Modeling Based On Multi-Conductor Transmission Line Model For Partial Discharge Study" journal of electrical Engineering & Technology (JEET), Vol. 9, No. 1, pp. 154-161, 2014.

S. M. Hassan Hosseini was born in Tehran, in 1969. He received his M.Sc. and Ph.D. degrees in electrical power engineering in 2000 and 2005 from Azad University South-Tehran Branch and Science & Research Branch, Tehran, Iran, respectively. His research interest is transient modeling of transformer, Partial Discharge, High Voltage Engineering, Electrical Insulation and Substation.

P. RezaeiBaravati was born in Tehran, in 1985. He received his M.Sc. degree in Electrical power Engineering from the Azad University South-Tehran Branch in 2013, His research interests include partial discharge measurement and localization in transformers, high frequency modeling of transformer windings and high frequency measurements on power transformers.